

A 4D Composite Higgs Model: Testing its Scalar Sector at the LHC

S. Moretti[†], A. Belyaev, M.S. Brown and D. Barducci

School of Physics & Astronomy, University of Southampton, Southampton SO17 1BJ, UK

S. De Curtis

INFN, Sezione di Firenze, Via G. Sansone 1, 50019 Sesto Fiorentino, ITALY

G.M. Pruna

*TU Dresden, Institut für Kern- und Teilchenphysik,
Zellescher Weg 19, D-01069 Dresden, GERMANY*

We explain the current Large Hadron Collider (LHC) data pointing to the discovery of a neutral Higgs boson in the context of a 4-Dimensional Composite Higgs Model (4DCHM). The full particle spectrum of this scenario is derived without any approximation and implemented in automated computational tools to enable fast phenomenological investigation. Several parameter configurations compliant with experimental constraints are presented and discussed. A χ^2 fit to the LHC data quantifying the consistency of the 4DCHM as a whole with experimental evidence is finally performed.

I. INTRODUCTION

The first question to ask following the discovery of a Higgs-like signal at the LHC by the ATLAS and CMS experiments [1, 2][39] would be whether such an object is fundamental or composite. After all, all (pseudo)scalar particles so far discovered in nature have been bound states of fermions. On the one hand, plenty of literature has ignored asking such a question and simply plunged into exploring the innumerable (and unquotable here) variations of the fundamental Higgs hypothesis. On the other hand, all those who did it eventually considered composite Higgs scenarios in some easily calculable regime, whereby the additional particle spectrum entering the ensuing models (generally comprising both new heavy gauge bosons and fermions) is essentially decoupled, i.e., by essentially accounting for the new heavy states in their infinite mass limit and studying the residual effects onto the SM sector. This may not be sufficiently accurate if one notices the following. Firstly, both species of new particles can affect the mixing pattern of the Higgs boson, modifying its couplings to the SM particles in a way that may depend on the new gauge boson and fermion masses. Secondly, they can appear as virtual objects interacting with the Higgs boson active at the LHC, if one realises that the Higgs production channel to which the LHC is most sensitive for a mass around 125 GeV is gluon-gluon fusion (which can occur in such models via not only loops of t , b quarks but also via t' , b' ones) and that the decay channel that appears most anomalous is the photon-photon one (which can occur in such models via not only loops of t , b quarks and W bosons but also via t' , b' and W' ones). Here too, if the masses of the new objects is not much larger than the Higgs mass, one should expect a dependence on these in the loop functions. In essence, it is clear that a more rigorous approach may be needed.

We followed this approach in Ref. [3] and we briefly report on it here. We will prove that the exact results can deviate from those obtained in the aforementioned decoupling limit of the new gauge and matter states, by adopting a particular composite Higgs model for which we have derived exactly the spectrum of particle masses and couplings which intervene at the LHC. Then, by exploiting the latter, we will explore the viability of the composite Higgs boson hypothesis at the LHC by comparing the corresponding predictions for cross sections and Branching Ratios (BRs) against the ATLAS and CMS data (herein we will neglect Tevatron results).

This write up is organised as follows. In Sect. II, we introduce the reference model adopted and briefly describe its Higgs sector. In Sect. III we map its allowed parameter space in the light of the latest experimental results. In Sect. IV we present our main findings. Finally, we conclude in Sect. V.

II. THE HIGGS SECTOR OF THE 4DCHM

The model we adopted for our analysis is the 4DCHM of [4], to which we refer for further details. Our main interest here will be the composite Higgs state and its couplings to both the SM particles (mainly to the W and Z gauge bosons plus the t and b quarks) and to the other new objects belonging to such model (the W' and Z' gauge bosons plus the t' and b' quarks). For a detailed phenomenological analysis of the gauge sector of the 4DCHM we refer to [5–7].

Neutral Gauge Bosons	$Z_{1,2,\dots,5}$
Charged Gauge Bosons	$W_{1,2,3}^{\pm}$
Charge 2/3 quarks	$T_{1,2,\dots,8}$
Charge $-1/3$ quarks	$B_{1,2,\dots,8}$
Charge 5/3 quarks	$\tilde{T}_{1,2}$
Charge $-4/3$ quarks	$\tilde{B}_{1,2}$

TABLE I: Extra particles of the 4DCHM with respect to the SM (an increasing particle number implies a larger mass).

The 4DCHM is an effective low-energy Lagrangian approximation that represents an extremely deconstructed version of the Minimal Composite Higgs model (MCHM) of [8] based on the coset $SO(5)/SO(4)$ that gives four Pseudo Nambu-Goldstone Bosons (PNGBs) in the vector representation of $SO(4)$, one of which is the (physical) composite Higgs boson, H . This extreme deconstruction of the 5D theory leads to a two site schematic representation, respectively called elementary and composite sectors (considered already in [9] where, however, the full gauge/Goldstone boson structure of the theory is not incorporated). Although extreme, this two site truncation represents the framework where to study in a computable way the lowest lying resonances (both bosonic and fermionic) that are the only ones that may be accessible at the LHC. In essence, the 4DCHM represents the ideal phenomenological framework where to test the idea of a composite Higgs boson as a PNGB (see also [10] although with a different construction).

The composite Higgs particle acquires mass, m_H , through a one-loop generated potential (à la Coleman-Weinberg). The particular choice for the fermionic sector of [4] gives a finite potential and from the location of the minimum one extracts the expression for m_H and its Vacuum Expectation Value (VEV), $\langle h \rangle$, in terms of the parameters of the model. Further, for a natural choice of these, the Higgs mass can be consistent with the recent results of the ATLAS [1] and CMS [2] experiments, measuring m_H around 125 GeV (as mentioned). Also for this reason then we will adopt the effective description of the 4DCHM for our phenomenological analysis of Higgs processes at the LHC. Finally, in the spirit of partial compositeness, spin 1 and spin 1/2 particles from the SM are coupled to the Higgs boson only via mixing with the corresponding composite particles while the new gauge and fermionic resonances directly interact with the Higgs field[40].

III. THE 4DCHM PARAMETER SPACE

Alongside the customary SM matter and force states (the e^- , μ^- , τ^- , $\nu_{e,\mu,\tau}$ leptons, the u , d , c , s , t , b quarks, the γ , Z , W^\pm , g gauge bosons), the 4DCHM incorporates the Higgs state H as a PNGB and a large number of new particles, both in the fermionic (quark) and bosonic (gauge) sector: see Tab. I.

To enable an efficient phenomenological analysis of the Higgs sector, we have implemented the 4DCHM in LanHEP [11], through the SLHA+ library [12], thereby deriving in an automated way the Feynman rules in CalcHEP format [13, 14]. In addition, we have listed in Tabs. 1 and 2 of Ref. [5] the correspondence between the model notations used here and in [3] and the ones uploaded onto the High Energy Physics Model DataBase (HEPMDB) [15] at <http://hepmdb.soton.ac.uk/hepmdb:0213.0123> under the name “4DCHM (with HAA/HGG)”.

To map the valid parameter space of the 4DCHM we have written a Mathematica routine [16], which considers f (the compositeness scale) and g_* (the coupling common to the non-SM gauge groups) as free parameters, performs scans over m_* , Δ_{tL} , Δ_{tR} , Y_T , M_{Y_T} , Δ_{bL} , Δ_{bR} , Y_B , M_{Y_B} (see [3] for their definition) and finds allowed points reproducing the following physical observables: e , M_Z , G_F , with values as per Particle Data Group (PDG) listing [17], $165 \text{ GeV} \leq m_t \leq 175 \text{ GeV}$, $2 \text{ GeV} \leq m_b \leq 6 \text{ GeV}$ and $124 \text{ GeV} \leq m_H \leq 126 \text{ GeV}$ [41]. Also notice that we have constrained the W^-tb , $Zt\bar{t}$ and $Zb\bar{b}$ couplings to data. Finally, regarding the latter, the program also checks that the left- and right-handed couplings of the Z boson to the bottom (anti)quark are separately consistent with results of LEP and SLC [18].

As mentioned, in the 4DCHM description, additional fermions belong to its spectrum, t' s and b' s, with SM-like charges. As these states are heavy quarks, they can in principle be produced in hadron-hadron collisions. The most stringent limits on their mass come at present from the LHC. To account for the latter, an analysis of the compatibility of the 4DCHM with LHC direct measurements has been performed. The pair production cross section $\sigma(pp \rightarrow t'\bar{t}'/b'\bar{b}')$ has been calculated according to the code described in [19]. Clearly, in the 4DCHM, such mass limits would apply to the lightest t' and b' states, i.e., T_1 and B_1 in Tab. I. Our limits on t' s are

	ATLAS	CMS
$R_{\gamma\gamma}$	1.8 ± 0.4	$1.564^{+0.460}_{-0.419}$
R_{ZZ}	1.0 ± 0.4	$0.807^{+0.349}_{-0.280}$
R_{WW}	1.5 ± 0.6	$0.699^{+0.245}_{-0.232}$
R_{bb}	-0.4 ± 1.0	$1.075^{+0.593}_{-0.566}$

TABLE II: LHC measurements of some R parameters from ATLAS [25] and CMS [26] data. (The CMS numerical values can actually be found in [27].)

based on [20], where a search for pair production of t 's is performed in CMS with 5 fb^{-1} of luminosity, where the t 's are assumed to decay 100% into W^+b , and on [21], where a search for pair production of t 's is performed at CMS with 1.14 fb^{-1} of luminosity, where the t 's are assumed to decay 100% into Zt . The limits on b 's are based on [22], where a search for pair production of b 's is performed at CMS with 4.9 fb^{-1} of luminosity with the b 's that are assumed to decay 100% into W^-t , and on [23], where a search for pair production of b 's is performed at CMS with 4.9 fb^{-1} of luminosity with the b 's that are assumed to decay 100% into Zb . Finally, notice that data considered here come from the 7 TeV run of the LHC. Results for T_1 and B_1 are shown in Figs. 1 and 2 of Ref. [3], respectively[42]. In practise, from the analysis, limits of about 400 GeV on both m_{T_1} and m_{B_1} can be ascertained.

However, one ought to notice that, beside the heavy fermions with ordinary charges, i.e., the t 's and b 's in our notation, the composite fermionic spectrum presents also states with exotic charge, as mentioned in the model description. Although these states do not couple directly to the Higgs boson, so that they are inert for our purposes here, it is important to set bounds on their masses since, in certain region of the parameter space, they can be almost degenerate with the lightest t' or b' . Since the fermionic spectrum is determined by the parameters we listed in Sect. II, it is clear that a bound on \tilde{T}_1 (the lightest fermion with charge $5/3$) mass reflects also on m_{T_1} and m_{B_1} . Regarding \tilde{T}_1 , since in the 4DCHM this particle decays almost 100% of the times into W^+t , it is possible to apply directly the bound of 650 GeV given by [24]. Nevertheless, there are regions of the fermion parameter space where the \tilde{T}_1 is not the lightest heavy fermion[43]. This means that the aforementioned values of m_{T_1} and m_{B_1} around 400 GeV remain valid.

The additional gauge bosons of the 4DCHM, the W 's and Z 's, are taken with masses and couplings compliant with experimental limits from both EW precision measurements and direct searches [5].

IV. RESULTS

In this section we compare the yield of the surviving points with the LHC data. To this end, a useful procedure to adopt is to define the so-called R (sometimes called μ) parameters, i.e., the observed signal (in terms of counted events) in a specific channel divided by the SM expectation:

$$R_{YY} = \frac{\sigma(pp \rightarrow HX)|_{\text{4DCHM}} \times \text{BR}(H \rightarrow YY)|_{\text{4DCHM}}}{\sigma(pp \rightarrow HX)|_{\text{SM}} \times \text{BR}(H \rightarrow YY)|_{\text{SM}}}, \quad (1)$$

where YY refers here to any possible Higgs decay channel and in our study we consider $YY = \gamma\gamma, b\bar{b}, WW$ and ZZ . The particles (if any) produced in association with the Higgs boson are here denoted by X [44]. For the latest experimental results on such quantities, wherein the label 4DCHM is meant to signify actual experimental data, see Tab. II.

The relevant (for current LHC data) hadro-production processes at partonic level are (here $V = W, Z$)

$$\begin{aligned} gg &\rightarrow H && (\text{gluon} - \text{gluon fusion}), \\ q\bar{q} &\rightarrow q\bar{q}H && (\text{vector boson fusion}), \\ q\bar{q}(') &\rightarrow VH && (\text{Higgs} - \text{strahlung}). \end{aligned} \quad (2)$$

For the purpose of our analysis, it is convenient to re-write eq. (1) as follows

$$R_{YY}^{Y'Y'} = \frac{\Gamma(H \rightarrow Y'Y')|_{\text{4DCHM}} \times \Gamma(H \rightarrow YY)|_{\text{4DCHM}}}{\Gamma(H \rightarrow Y'Y')|_{\text{SM}} \times \Gamma(H \rightarrow YY)|_{\text{SM}}} \frac{\Gamma_{\text{tot}}(H)|_{\text{SM}}}{\Gamma_{\text{tot}}(H)|_{\text{4DCHM}}}, \quad (3)$$

where $Y'Y'$ denotes incoming particles participating the Higgs boson production, e.g., gg for the first process and VV for the other processes in eq. (2), while YY indicates particles into which the Higgs boson decays[45].

For $YY = \gamma\gamma, WW, ZZ$ we take the dominant production process to be gluon-gluon fusion (i.e., $Y'Y' = gg$) while for $YY = b\bar{b}$ we assume that Higgs-strahlung dominates (i.e., $Y'Y' = VV$, with the appropriate superposition of WW and ZZ). In other words, we trade a cross section for a width (so-to-say) and this is possible, as we will be carrying out our analysis at lowest order without the presence of radiative corrections due to either Quantum Chromo-Dynamics (QCD) or EW interactions. In fact, following Ref. [28], we can cast eq. (3) also in the following form:

$$R_{YY}^{Y'Y'} = \frac{\kappa_{Y'}^2 \kappa_Y^2}{\kappa_H^2}, \quad (4)$$

wherein (recall that $VV = WW$ or ZZ and notice that $Y, Y' = b/\tau/g/\gamma/V$)

$$\kappa_{b/\tau/g/\gamma/V}^2 = \frac{\Gamma(H \rightarrow b\bar{b}/\tau^+\tau^-/gg/\gamma\gamma/VV)|_{4\text{DCHM}}}{\Gamma(H \rightarrow b\bar{b}/\tau^+\tau^-/gg/\gamma\gamma/VV)|_{\text{SM}}}, \quad (5)$$

$$\kappa_H^2 = \frac{\Gamma_{\text{tot}}(H)|_{4\text{DCHM}}}{\Gamma_{\text{tot}}(H)|_{\text{SM}}}. \quad (6)$$

The LHC experiments then perform fits to the κ_i coefficients in order to test generic Beyond the SM (BSM) assumptions (for which one or more of the the κ_i s can differ from 1). However, they generally fix $\kappa_H^2 = 1$, thereby assuming that the Higgs width does not change [25, 26][46]. This is a rather restrictive condition since most BSM models predict $\kappa_H^2 \neq 1$, as the Higgs boson under consideration can mix, in such BSM scenarios, directly with other Higgs boson states or, else, the particles to which it couples can in turn mix. Such effects, whichever their nature, would induce the condition $\kappa_H < 1$, as it is the case in the 4DCHM. In fact, we will show later on that many of the 4DCHM effects enter through such a modification of the Higgs total width.

In order to illustrate the 4DCHM phenomenology, we adopt as reference point the combination $f = 1$ TeV and $g_* = 2$. However, the salient features extracted for this case may equally be referred to the other benchmark points to be considered, i.e., those defined in Ref. [5]. Since the errors in Tab. II on $b\bar{b}$ are very large, Fig. 1 shows the correlation between the event rate ratios of eq. (3) only for the $\gamma\gamma$ and VV channels[47]. Furthermore, as intimated, since most of the sensitivity of the $\gamma\gamma$ and VV data is to the gluon-gluon fusion production mode, which is in fact the dominant one in the 4DCHM for the parameter space tested here, like for the SM, we will neglect the effects of all others in our predictions (so that we can conveniently drop the superscripts gg and VV for the time being), except for the $b\bar{b}$ decay channel (accessible via Higgs-strahlung), that we will consider later on. From the plot in Fig. 1 it is clear that there is a noticeable tendency of the model to prefer $R_{\gamma\gamma}$ and R_{VV} values smaller than 1 (the majority of points satisfy this condition, $R_{\gamma\gamma}$ being somewhat larger than R_{VV}), with WW showing a slightly stronger propensity than R_{ZZ} in this direction. The two plotted quantities also appear to be strongly correlated, thereby hinting at a possible common origin for the 4DCHM event rate behaviour relative to the SM predictions. Moreover, it is also worth mentioning here that the rates for R_{VV} in both the 4DCHM and the SM are computed for the gauge boson decay patterns which ATLAS and CMS used in reporting the results in Tab. II. These signatures include electrons and muons in all possible combinations entering generic ‘two-lepton plus missing transverse energy’ and ‘four-lepton’ signatures emerging from WW and ZZ pairs, respectively[48]. In addition, we have checked that the contribution of W' and Z' states, two of the former and three of the latter, to the yield of these final states, in both mixed 4DCHM/SM and pure 4DCHM channels, is negligible, owing to their large masses as compared to the SM gauge states W and Z , despite their large couplings.

It is now useful to unfold the results in Fig. 1 in terms of the three κ_i^2 entering eq. (4), as each of these can be an independent source of variation in the 4DCHM with respect to the SM. In particular, we map such results in terms of the masses of the lightest t' and b' quarks, i.e., T_1 and B_1 , as these are the 4DCHM quantities to which the event rate ratios are most sensitive.

We start with κ_H^2 . This is shown in Fig. 2. Herein, we keep all generated 4DCHM points, including those failing the constraints from direct searches for t' , b' states or the exotic 5/3 charged fermion. This is done for the purpose of illustrating the aforementioned sensitivity of the 4DCHM predictions upon the heavy top and bottom masses. In fact, should have smaller m_{T_1} and m_{B_1} been allowed, effects onto the ratio of total widths would have been extremely large, up to -30% or so. However, even with the aforementioned limits enforced, the 4DCHM effects induced by t' and b' states onto the SM remain substantial, of order -15% to -20% . Hence, bearing in mind that the contribution of the $H \rightarrow gg, \gamma\gamma$ and $Z\gamma$ partial widths (those where such t' and

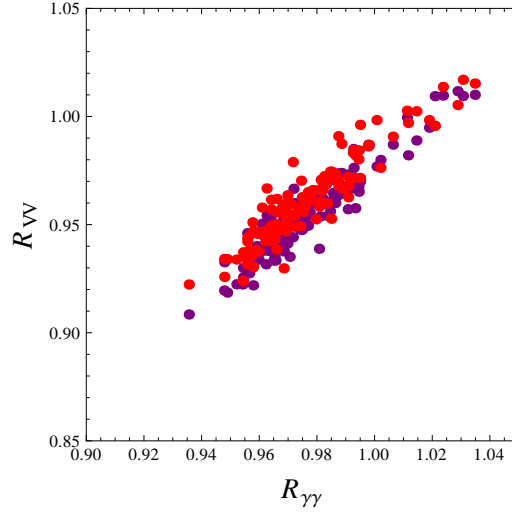


FIG. 1: Correlation between $R_{\gamma\gamma}$ and R_{VV} , with $VV = WW$ (red) and ZZ (purple), from eq. (3) in the 4DCHM for the benchmark point $f = 1$ TeV and $g_* = 2$. All points generated here are compliant with direct searches for t' s, b' s and exotic states with charge $5/3$.

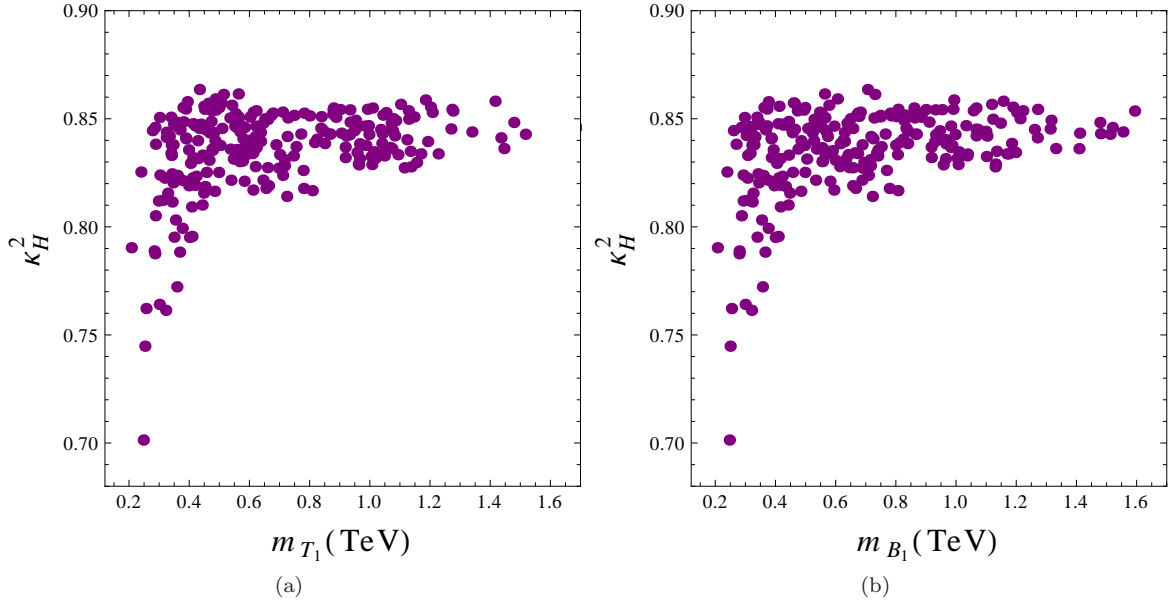


FIG. 2: The distributions of κ_H values entering eq. (4) as a function of (a) m_{T_1} and (b) m_{B_1} in the 4DCHM for the benchmark point $f = 1$ TeV and $g_* = 2$.

b' states enter at lowest order) to the total one are negligible, one has to conclude that these corrections are induced by mixing effects. Furthermore, as $\Gamma_{\text{tot}}(H)|_{4\text{DCHM}} \approx \Gamma(H \rightarrow b\bar{b})|_{4\text{DCHM}}$ (just like in the SM), it is also clear that these are mainly due to b' - b mixing affecting the $Hb\bar{b}$ coupling. Therefore, the result that such 4DCHM effects are negative is not surprising. Overall, the reduction of the total Higgs width in the 4DCHM with respect to the SM induces an increase of all R values in eq. (3) except, of course, $R_{b\bar{b}}$.

Since we are interested in probing the 4DCHM hypothesis as an explanation of the LHC data used for the Higgs search and since the largest anomaly with respect to the SM is seen in the di-photon channel (recall Tab. II), we next study κ_g^2 and κ_γ^2 , also entering eq. (4)[49]. We show these two quantities in Figs. 3–4, respectively. In both cases, we see a reduction of the partial widths in the 4DCHM relative to the SM. Again, we trace this to mixing effects, this time between t and t' states. Both at production and decay level, in fact, t contributions are larger than the b ones, both in the 4DCHM and SM. Again, they induce negative corrections,

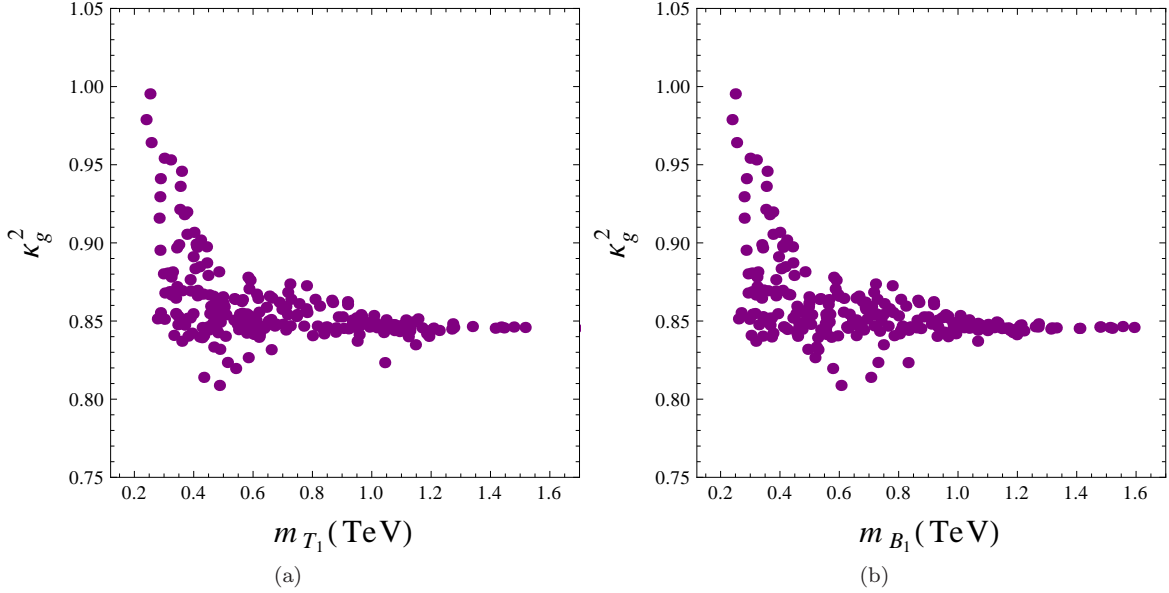


FIG. 3: The distributions of κ_g values entering eq. (4) as a function of (a) m_{T_1} and (b) m_{B_1} in the 4DCHM for the benchmark point $f = 1$ TeV and $g_* = 2$.

typically -10% for κ_g and -6% for κ_γ . Furthermore, that the former are larger than the latter is due to the fact that the t loop is the leading one in the production graph whereas it is subleading (smaller than the W contribution) in the decay diagram. Incidentally, unlike the case of the total width, for these two partial widths, if lighter T_1 and B_1 masses were allowed (they are strongly correlated), genuine 4DCHM effects onto the SM would have been different in the two channels, typically inducing larger(smaller) rates at production(decay) level. In this dynamics we recognise the effects of the t' and b' loops in the two triangle amplitudes (as opposed to those induced by mixing in the couplings). In fact, the lighter the t' and b' masses, the bigger their loop contributions[50]. So that, at both production and decay level, the net effect from t' and b' loops turn out to have the same sign as the t one (recall that the b ones are negligible in both models) for the case of a light T_1 or B_1 (below 500 GeV). Hence, in production they interfere constructively with the leading t contribution, which in turn means that they interfere destructively in decay with the leading W contribution (which has a sign opposite to the t term). In case of a heavier T_1 and B_1 , the sign of the overall contribution of t' and b' quarks can vary with respect to the top quark one but the combined contribution of all heavy quarks is quite small. In fact, we have verified that the asymptotic values, i.e., for large m_{T_1} and m_{B_1} , attained by κ_g^2 and κ_γ^2 in Figs. 3 and 4, respectively, coincide with those obtained in the aforementioned literature by adopting the described decoupling approximation of the heavy fermionic states. Conversely, it should be noted that the asymptotic results can differ significantly from those obtained for small T_1 and B_1 masses, particularly for κ_g^2 , up to 7% or so (around 400 GeV). For smaller masses, the effect would be even more prominent.

To summarise then, we are in presence of contrasting effects entering eq. (4). All κ_i^2 therein tend to diminish, relative to the SM. However, the decrease of κ_H^2 entering the denominator is bigger than the decrease of the $\kappa_Y^2 \times \kappa_{Y'}$ product in the numerator, so that the net effect could be the increase of the event rate in comparison to the SM. This dynamics was indeed shown in Fig. 1 while its details can be seen in Figs. 2–4.

In Fig. 5 we investigate these effects further for $R_{\gamma\gamma}$, for which (recall) the largest anomaly is seen, plotted as a function of m_{T_1} and m_{B_1} . For m_{T_1} and m_{B_1} above 400 GeV, $R_{\gamma\gamma}$ values can reach 1.1. However, again, should heavy quark masses be allowed to be below 400 GeV or so, the values for $R_{\gamma\gamma}$ could have been rather large, up to 1.2 (or even more). In fact, quite irrespectively of the actual values attained by $R_{\gamma\gamma}$, the tendency in Fig. 5 is clear enough. There is a consistent ‘leakage’ of points towards $R_{\gamma\gamma} > 1$, the more so the lighter m_{T_1} and m_{B_1} . The relevance of this result is twofold. On the one hand, this calls for a thorough re-examination from an experimental point of view of the actual limits on the t' and b' states, especially for low masses, certainly affording an accuracy well beyond the one stemming from the rudimentary approach we have adopted in Figs. 1–2 of Ref. [3]. On the other hand, we would like to argue that statements from previous literature, mentioning that accurate predictions can be made in the infinite t' and b' mass limit [29–32], may not be applicable to our concrete realisation of the 4DCHM.

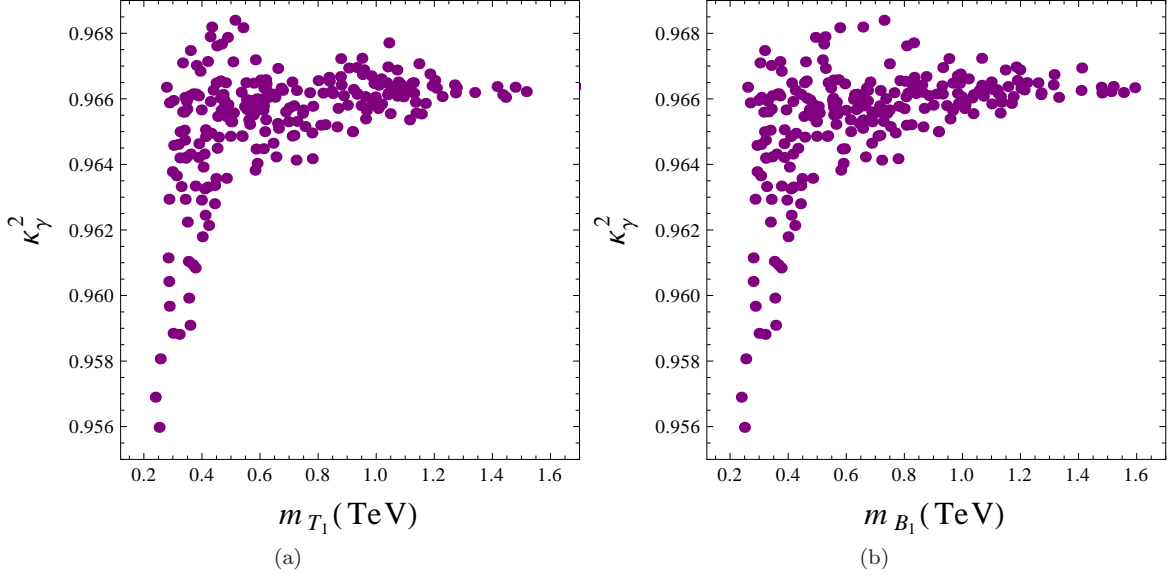


FIG. 4: The distributions of κ_γ values entering eq. (4) as a function of (a) m_{T_1} and (b) m_{B_1} in the 4DCHM for the benchmark point $f = 1$ TeV and $g_* = 2$.

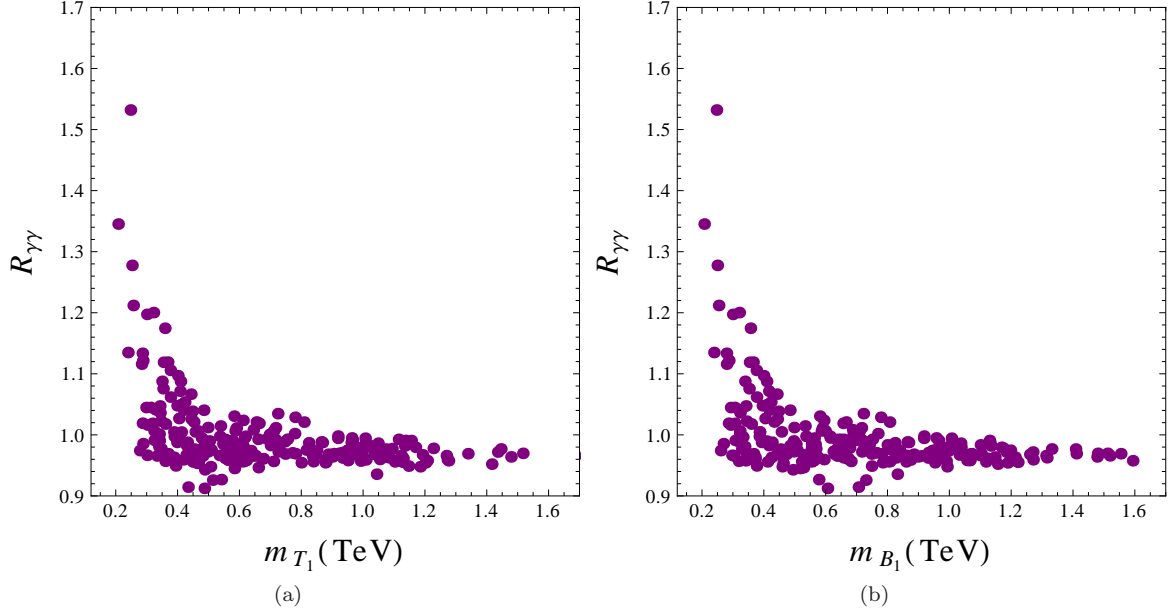


FIG. 5: The distributions of $R_{\gamma\gamma}$ values entering eq. (3) as a function of (a) m_{T_1} and (b) m_{B_1} in the 4DCHM for the benchmark point $f = 1$ TeV and $g_* = 2$.

However, for the time being, we take the limits on m_{T_1} and m_{B_1} as we obtained them at face value and collect all the results produced, including those for the other f and g_* benchmarks, and compare them to the experimental results of ATLAS [25] and CMS [26] collected in Tab. II.

For each (f, g_*) benchmark we scan over the other free parameters and remove points that do not survive the t' , b' and charge 5/3 quark direct search constraints. For the remaining points we calculate R_{YY} for $YY = \gamma\gamma$, WW , ZZ , $b\bar{b}$. The results are shown in Fig. 6(a) as a series of normalised histograms in order to demonstrate the number of points in the scan taking particular values of R_{YY} and the full range of values obtained is shown. The experimental measurements for R_{YY} are shown by black and white points with 68% Confidence Level (CL) error bars. As the scale f is increased, the values of R_{YY} become more sparse. This is because parameters in

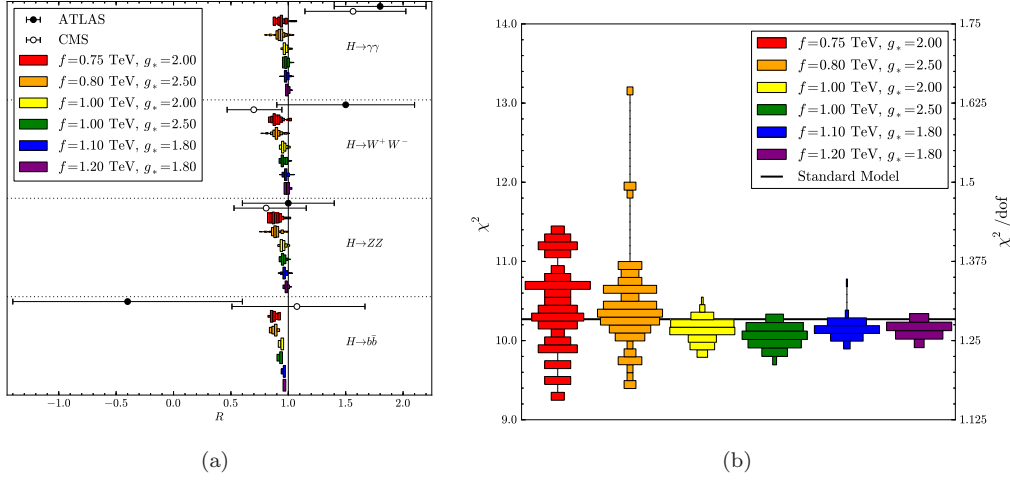


FIG. 6: (a) Comparison of the R 's from eq. (3) with the measured experimental values by ATLAS [25] and CMS [26] (see Tab. II) in the 4DCHM for all benchmark points in f and g_* . (b) The χ^2 fit (as described in the text) in the 4DCHM for all benchmark points in f and g_* . All points generated here are compliant with direct searches for t 's, b 's and exotic states with charge $5/3$.

the model become more tightly constrained as this scale grows larger.

In order to have a clear picture on how the 4DCHM fares against LHC data, particularly in relation to the SM, in a quantitative way, we calculate the χ^2 goodness of our fit for the ATLAS [25] and CMS [26] data from Tab. II. We assume that all the channels and experiments are independent and simply sum them in the χ^2 function, giving us eight degrees of freedom (dof). The value of χ^2 for each parameter scan point (surviving the experimental constraints discussed above) is shown in Fig. 6(b) using normalised histograms. The value of our χ^2 function for the SM (i.e., $R_{\gamma\gamma} = 1$) is also plotted as a horizontal black line and the figure makes it clear that the 4DCHM represents a better fit to the data than the SM does for most of the benchmarks considered.

V. CONCLUSIONS

In summary, we have shown that the 4DCHM could provide an alternative (at times even better) explanation than the SM of the current LHC data pointing to the discovery of a neutral Higgs boson with mass around 125 GeV.

After systematically scanning the parameter space of the 4DCHM and illustrating its phenomenology for several benchmark points, we have shown that a moderate enhancement in the $H \rightarrow \gamma\gamma$ channel with respect to the SM predictions is a possible feature of this model and can be as large as about 1.1, somewhat below the central values of the experimental measurements.

However, we have also found that this enhancement could potentially be larger, realistically up to 1.3, due to the contribution from the heavy t' and b' fermions of the 4DCHM with mass just below 400 GeV, i.e., precisely when entering mass regions apparently excluded but for which there are no data from direct searches, only simple extrapolations that we attempted here. So, a thorough re-assessment from the experimental side is required in this respect[51].

The main source of the enhancement of the $H \rightarrow \gamma\gamma$ channel is in the reduction of the $H \rightarrow b\bar{b}$ partial width due to b - b' mixing effects which in turn leads to the reduction of the total Higgs boson width and the enhancement of all decay channels, including the di-photon one. Competing effects emerge though from the (effective) Hgg coupling becoming simultaneously smaller.

Finally, a relevant by-product of our analysis has been to show that several approximations adopted in literature in scenarios similar to the 4DCHM, which essentially make predictions in the limit in which the masses of the heavy fermions (and possibly heavy gauge bosons) are infinitely heavy, cannot generally be accurate over the entire parameter space of the corresponding model.

Acknowledgments

SM is grateful to the workshop organisation for financial support and for a stimulating and entertaining meeting. DB, AB and SM are financed in part through the NExT Institute. The work of GMP has been supported by the German Research Foundation DFG through Grant No. STO876/2-1 and by BMBF Grant No. 05H09ODE.

-
- [1] G. Aad et al. (ATLAS Collaboration), Phys. Lett. **B716**, 1 (2012), 1207.7214.
 - [2] S. Chatrchyan et al. (CMS Collaboration), Phys. Lett. **B716**, 30 (2012), 1207.7235.
 - [3] D. Barducci, A. Belyaev, M. Brown, S. De Curtis, S. Moretti, et al. (2013), 1302.2371.
 - [4] S. De Curtis, M. Redi, and A. Tesi, JHEP **1204**, 042 (2012), 1110.1613.
 - [5] D. Barducci, A. Belyaev, S. De Curtis, S. Moretti, and G. M. Pruna (2012), 1210.2927.
 - [6] D. Barducci, L. Fedeli, S. Moretti, S. De Curtis, and G. M. Pruna (2012), 1212.4875.
 - [7] D. Barducci, S. De Curtis, K. Mimasu, and S. Moretti (2012), 1212.5948.
 - [8] K. Agashe, R. Contino, and A. Pomarol, Nucl. Phys. **B719**, 165 (2005), hep-ph/0412089.
 - [9] R. Contino, T. Kramer, M. Son, and R. Sundrum, JHEP **0705**, 074 (2007), hep-ph/0612180.
 - [10] G. Panico and A. Wulzer, JHEP **1109**, 135 (2011), 1106.2719.
 - [11] A. Semenov (2010), 1005.1909.
 - [12] G. Belanger, N. D. Christensen, A. Pukhov, and A. Semenov, Comput. Phys. Commun. **182**, 763 (2011), 1008.0181.
 - [13] A. Pukhov, E. Boos, M. Dubinin, V. Edneral, V. Ilyin, et al. (1999), hep-ph/9908288.
 - [14] A. Belyaev, N. D. Christensen, and A. Pukhov (2012), 1207.6082.
 - [15] M. Bondarenko et al. (2012), 1203.1488.
 - [16] *Mathematica Edition: Version 7.0* (Wolfram Research, Inc., Champaign, Illinois, 2008).
 - [17] The Particle Data Group, <http://pdg.lbl.gov/>.
 - [18] The ALEPH, DELPHI, L3, OPAL, SLD Collaborations, the LEP Electroweak Working Group, the SLD Electroweak and Heavy Flavour Groups, Phys. Rept. **427**, 257 (2006), hep-ex/0509008.
 - [19] M. Cacciari, M. Czakon, M. Mangano, A. Mitov, and P. Nason, Phys. Lett. **B710**, 612 (2012), 1111.5869.
 - [20] S. Chatrchyan et al. (CMS Collaboration), Phys. Lett. **B716**, 103 (2012), 1203.5410.
 - [21] S. Chatrchyan et al. (CMS Collaboration), Phys. Rev. Lett. **107**, 271802 (2011), 1109.4985.
 - [22] S. Chatrchyan et al. (CMS Collaboration), JHEP **1205**, 123 (2012), 1204.1088.
 - [23] CMS Collaboration, S. Chatrchyan *et al.*, CMS-PAS-EXO-11-066.
 - [24] Tech. Rep. ATLAS-CONF-2012-130, CERN, Geneva (2012).
 - [25] Tech. Rep. ATLAS-CONF-2012-170, CERN, Geneva (2012).
 - [26] Tech. Rep. CMS-PAS-HIG-12-045, CERN, Geneva (2012).
 - [27] CMS Higgs TWiki, <https://twiki.cern.ch/twiki/bin/view/CMSPublic/Hig12045TWiki>.
 - [28] A. David, A. Denner, M. Duehrssen, M. Grazzini, et al. (2012), 1209.0040.
 - [29] A. Azatov and J. Galloway, Phys. Rev. **D85**, 055013 (2012), 1110.5646.
 - [30] A. Azatov, R. Contino, D. Del Re, J. Galloway, M. Grassi, et al., JHEP **1206**, 134 (2012), 1204.4817.
 - [31] M. Gillioz, R. Grober, C. Grojean, M. Muhlleitner, and E. Salvioni, JHEP **1210**, 004 (2012), 1206.7120.
 - [32] A. Azatov, R. Contino, and J. Galloway (2012), 1206.3171.
 - [33] T. Aaltonen et al. (CDF Collaboration, D0 Collaboration), Phys. Rev. Lett. **109**, 071804 (2012), 1207.6436.
 - [34] S. Chatrchyan et al. (CMS Collaboration), Phys. Lett. **B718**, 307 (2012), 1209.0471.
 - [35] S. Chatrchyan et al. (CMS Collaboration) (2012), 1210.7471.
 - [36] M. Spira, A. Djouadi, D. Graudenz, and P. Zerwas, Nucl. Phys. **B453**, 17 (1995), hep-ph/9504378.
 - [37] Z. Kunszt, S. Moretti, and W. J. Stirling, Z. Phys. **C74**, 479 (1997), hep-ph/9611397.
 - [38] Tech. Rep. ATLAS-CONF-2013-018, CERN, Geneva (2013).
 - [39] Some supplemental evidence also emerged at the Tevatron [33].
 - [40] In the 4DCHM, regarding the fermionic sector, only the top and bottom quarks are mixed with the composite fermions.
 - [41] Notice that m_t and m_b in composite Higgs models have to be run down from the composite scale, so that their mass intervals adopted reflect the uncertainties entering such an evolution.
 - [42] More recent results from CMS are given in [34] and [35], however, they will not change our conclusions.
 - [43] In contrast, we have to say that, at the moment, no limits for the charge $-4/3$ fermions are given by the ATLAS and CMS collaborations. They will of course further cut on the low mass values for T_1 and B_1 .
 - [44] In reality, one should notice that eq. (1) is the limiting case in which sensitivity to the YY decay channel is through only one of the production processes [36, 37]. One should more accurately sum over all of the latter. However, given present data samples and for our purposes, such an approximation is accurate enough.

- [45] Notice that the coupling between the Higgs boson and W or Z intervening in the last two production channels in (2) is the same. However, also notice that, in the 4DCHM, the two couplings HWW and HZZ do not rescale in the same way with respect to the SM ones, in particular for the parameter space investigated here, though the differences will be shown to be small. Hereafter, we will adopt the generic label V to signify either a W or a Z .
- [46] In fact, the only departure from this they allow for is to take $\kappa_H^2 > 1$, corresponding to a value of the Higgs total width in the BSM hypothesis larger than in the SM case, thus accounting for, e.g., invisible Higgs decays that are not captured by standard searches.
- [47] However, the $b\bar{b}$ case will be taken into consideration later on when making fits to data. In contrast, the $\tau^+\tau^-$ case, being even worse in the above respect, is ignored throughout.
- [48] This clarification is of relevance for the case of the 4DCHM, in which the W and Z decay rates change relatively to the SM, unlike the case of other popular BSM models.
- [49] The case of κ_V^2 is relevant too, as also the HVV couplings in the 4DCHM change from their SM values (and, as mentioned, differently for WW and ZZ). However, here, the dynamics occur at tree-level, so the effects are trivial, as they can be easily accounted for by replacing the HVV couplings of the SM with those of the 4DCHM. Needless to say, also in this case the differences between SM and 4DCHM are negative and due to mixing, which is non-negligible.
- [50] Also recall that the $Ht'\bar{t}'$ and $Hb'\bar{b}'$ couplings are not of Yukawa type, that is, they do not scale linearly with the t' and b' masses.
- [51] After the release of [3], we have become aware that some experimental work in this direction has started [38], which, however, does not change the main conclusions of this paper.